

## Article

# Capacity Enhancement Analysis of an OAM-OFDM-SMM Multiplexed Free Space Communication System in Atmospheric Turbulence

Shivaji Sinha <sup>1</sup>, Chakresh Kumar <sup>1,\*</sup>, Ammar Armghan <sup>2</sup>, Mehtab Singh <sup>3</sup>, Meshari Alsharari <sup>2</sup>  
and Khaled Aliqab <sup>2,\*</sup>

<sup>1</sup> University School of Information, Communication & Technology, Guru Gobind Singh Indraprastha University, Sector 16 C, Dwarka, New Delhi 110078, India

<sup>2</sup> Department of Electrical Engineering, College of Engineering, Jouf University, Sakaka 72388, Saudi Arabia

<sup>3</sup> Department of Electronics and Communication Engineering, University Institute of Engineering, Chandigarh University, Mohali 140413, India

\* Correspondence: chakreshk@ipu.ac.in (C.K.); kmaliqab@ju.edu.sa (K.A.)

**Abstract:** To overcome atmospheric turbulence (AT) distortion during signal propagation through the optical link, orbital angular momentum (OAM) mode states employing multiple inputs and multiple outputs (MIMO) techniques have recently gained prominence in free space optical communication (FSO). As the various OAM modes propagate through the free space optical link, signal attenuation and crosstalk may occur, reducing system capacity and increasing the likelihood of bit errors. In this work, our objective is to propose a spectrally efficient, high-speed and channel capacity efficient crosstalk FSO communication system by combining the features of orthogonal frequency division multiplexing (OFDM), spatial mode multiplexing (SMM), and a mode diversity scheme into an existing OAM-FSO communication system. The incorporation of the OFDM-MIMO concept and spatial mode diversity into the existing OAM-MIMO-FSO system is extremely beneficial in enhancing the transmission capacity, mitigating multipath fading and atmospheric turbulence distortions. The Gamma–Gamma (GG) model is used to assess the performance of the proposed system under various atmospheric turbulence conditions in terms of the performance metrics such as BER vs. number of OAM states for different refractive index structure and Rytov constants, link distance, and an optical signal to noise ratio (OSNR). A FEC limit of  $3.8 \times 10^{-3}$  and a maximum link distance of 2 km are set to evaluate these performance parameters. Finally, the transmission capacity of the proposed system is compared to that of the existing MIMO and OAM-SMM-MIMO systems for different OSNR values under atmospheric turbulence conditions for the OAM state of  $l = +1$ , yielding an overall improvement of 3.3 bits/s/Hz compared to conventional MIMO systems and 1.6 bits/s/Hz for the OAM-SMM-MIMO system.

**Keywords:** adaptive MIMO equalization; bit error rate (BER); orbital angular momentum multiplexing; optical signal to noise ratio (OSNR); orthogonal frequency division multiplexing (OFDM); quadrature amplitude modulation (QAM); free space optical communications (FSO); spatial mode multiplexing (SMM); spatial mode diversity (SMD)



**Citation:** Sinha, S.; Kumar, C.; Armghan, A.; Singh, M.; Alsharari, M.; Aliqab, K. Capacity Enhancement Analysis of an OAM-OFDM-SMM Multiplexed Free Space Communication System in Atmospheric Turbulence. *Appl. Sci.* **2023**, *13*, 3897. <https://doi.org/10.3390/app13063897>

Academic Editors: Amalia Miliou and Sergio Toscani

Received: 24 December 2022

Revised: 12 March 2023

Accepted: 16 March 2023

Published: 19 March 2023



**Copyright:** © 2023 by the authors. Licensee MDPI, Basel, Switzerland. This article is an open access article distributed under the terms and conditions of the Creative Commons Attribution (CC BY) license (<https://creativecommons.org/licenses/by/4.0/>).

## 1. Introduction

Increasing system capacity and optimizing spectral efficiency in free space optical communication (FSO) is a major challenge. To address these challenges, we must adopt a new degree of flexibility in our approach in order to improve transmission capacity and spectrum efficiency [1].

Orbital angular momentum (OAM) technology, which uses twisted light beams with spiral spatial structure and an infinite number of natural orthogonal states, has received much attention in free space communication in recent years. By choosing suitable OAM

mode multiplexing, a high-capacity and spectrally efficient FSO system can be developed using these intrinsic orthogonal states [2]. When this OAM technology is integrated with orthogonal frequency division multiplexing (OFDM), along with a mode diversity scheme, the capacity of the FSO link can be further improved. However, the transmission of OAM-OFDM multiplexed spatial beams through the atmospheric turbulence (AT) channel has rarely been investigated and studied in the literature. Hence, it is a key issue to analyze the impact of AT on the capacity of the transmitted OAM-OFDM multiplexed signal during propagation [3].

OAM multiplexing has been successfully implemented with a spectral efficiency of 95.7 bps/Hz and a system capacity of 2.56 Tbps by Wang et al. [4] at 193.4 THz in the optical domain. A channel capacity of 100.8 Tb/s has been achieved in Huang et al. [5] by incorporating OAM and polarization with wavelength division multiplexing (WDM) techniques. To achieve this high transmission capacity, the proposed system has successfully transmitted a total of 12 OAM channels, with each channel carrying out 100 Gbps of QPSK-modulated data at two different polarizations over 42 different wavelengths.

A new approach to OAM beams using spatial modulation (SM) based millimeter wave communication systems, which employ spatial distribution characteristics, has been proposed to achieve a 341.6% improvement in energy efficiency over MIMO systems. The system performance has been analytically evaluated using performance metrics such as capacity, average bit error probability, and energy efficiency and has been identified as robust against path loss attenuation and suitable for long range transmission [6].

L. Wang et al. [7] have proposed and analytically evaluated the performance of the capacity model of an OAM based MIMO wireless communication system. The simulation results showed that the OAM-MIMO wireless model outperformed conventional OAM and MIMO transmission systems in terms of transmission capacity over a long transmission range.

The simultaneous transmission of spatially orthogonal and OAM multiplexed signals through a single aperture pair has evolved as a novel method to increase the transmission capacity by multiple folds with minimal crosstalk [8]. The proposed system has been designed to investigate the power loss and channel crosstalk of the link in the case of limited-size receiver apertures, as well as pointing and lateral errors between the transmitter and receiver [8].

G. Xie, L. Li, et al. [9] have demonstrated a single aperture based, eight-OAM multiplexed FSO system. At a BER threshold of  $3.8 \times 10^{-3}$ , 32 Gbps of multiple coaxial information was transmitted over a 2.5-m link distance to achieve a spectral efficiency of 16 bit/s/Hz with crosstalk less than  $-12.5$  dB.

Ref. [10], which has been investigated for crosstalk mitigation issues, is a  $4 \times 4$  OAM-MIMO FSO system using adaptive equalization techniques employing heterodyne detection. Each OAM channel has transmitted a 20 Gbps QPSK signal under weak turbulence conditions. The numerical results demonstrate that the signal quality can be improved by using MIMO processing techniques, which help in reducing the power penalty by greater than 4 dB at a threshold BER of  $3.8 \times 10^{-3}$ .

In the article [11], the advantages of MIMO based spatial multiplexing technique have been incorporated in OAM multiplexing to increase the FSO system capacity. A  $2 \times 2$  aperture architecture, where each transmitter aperture transmits two multiplexed OAM beams, has been proposed to design an 80 Gbps FSO system. The result obtained shows the power penalty to be less than 3.6 dB at the BER limit of  $3.8 \times 10^{-3}$ .

Incorporating multiple aperture sizes in MIMO based multiple OAM using spatial mode multiplexing (SMM) has been widely investigated by different researchers to enhance the channel capacity and mitigate the turbulence-induced power fluctuations. However, in a practical FSO link, the design complexity, cost, and real-time processing capability of such an adaptive optical receiver remain critical issues [12,13]. The spiral wave-front of the OAM beams is susceptible to free space turbulence, resulting in inter-channel crosstalk (ICC) issues and the spreading of the power of the transmitted OAM states into different adjacent OAM states [14]. To maximize the capacity of the FSO link, such crosstalk has been thoroughly studied for Laguerre–Gaussian beams under various atmospheric turbulence scenarios for adaptive optic systems based on adaptive MIMO techniques [15].

In this research paper, an OAM-OFDM based spatial mode multiplexed (SMM) MIMO-FSO system design is presented, and the system performance is evaluated under different weak to strong atmospheric channel conditions. The spatial mode diversity (SMD) based MIMO signal processing scheme is proposed to improve the system's robustness against channel path loss attenuation and also to enhance the transmission capacity. By combining the benefits of OFDM and OAM multiplexing, the proposed design is not only made spectrally efficient and robust against the impact of multipath fading, but it also increases the proposed system's transmission capacity in the FSO link. This work presents 20 symmetrical hybrid spatially multiplexed (OAM-OFDM) orthogonal channels, each carrying 120 Gbps of 16-QAM modulated data at a wavelength of 1550 nm over a link distance of 2 km. When this hybrid spatially multiplexed signal is transmitted through the turbulence channel, the OAM mode state intensity profile and phase structure are distorted due to mode energy spreading to adjacent OAM states. The proposed system design BER performance is investigated under turbulent channel metrics such as the refractive index structure parameter, Rytov variance constant, and link distance. The BER performance is also compared for different transmitting OAM mode states in different turbulence conditions. The BER and the channel capacity performances of the proposed OAM-OFDM-SMM MIMO FSO system is investigated and compared by taking into consideration the MIMO and OAM-MIMO FSO systems as a function of OSNR in turbulent atmospheric conditions. Moreover, the analytical results illustrate that the BER of the OAM-OFDM-SMM MIMO FSO system decreases exponentially with an increase in OSNR values and significant improvement is observed at 20 dB OSNR. In addition, the channel capacity of the proposed system increases exponentially with an increase in OSNR and at OSNR of 18 dB, the capacity of the proposed system is improved by 3.3 bits/s/Hz compared to the other two FSO systems discussed above. The subsequent sections of this paper are organized as discussed below.

In Section 2, we have described the schematic design model of the proposed OAM-OFDM-SMM multiplexed free space communication system with detailed mathematical analysis, whereas the principle of the spatial mode diversity used in the proposed system is explained in Section 3. The mathematical concepts of the generation of the 16-QAM modulated SMM multiplexed OAM beam using a spatial phase mask (SPM) technique and its electric field distribution is discussed in this section. Moreover, the channel capacity model of the proposed system under the impact of the GG atmospheric turbulence condition is reported in Section 4. The numerical results obtained for the proposed system are investigated and analyzed in Section 5, whereas the final conclusions of the findings and potential future improvements of this research are summarized at the end of this paper in Section 6.

## 2. Proposed System Schematic Model

Figure 1 depicts the concept and working principle of the OAM based spatial multiplexed FSO system model, while Figure 2 illustrates the detailed experimental setup of the proposed OAM-OFDM-SMM-MIMO spatial multiplexed FSO system, which incorporates OFDM and adaptive SMM and SMD multiplexing schemes.

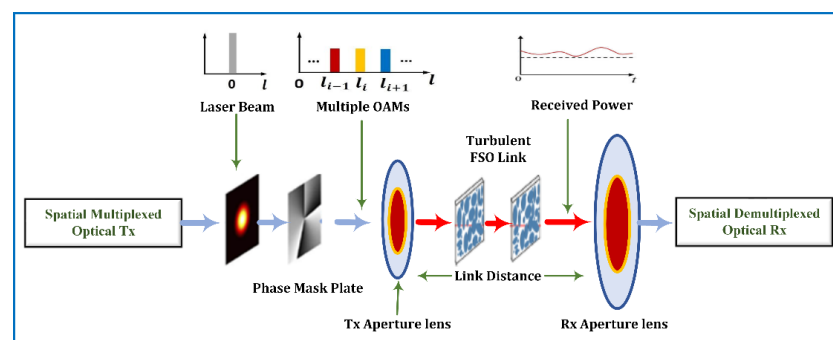


**Figure 1.** Schematic concept of OAM based spatial multiplexing in the FSO system.

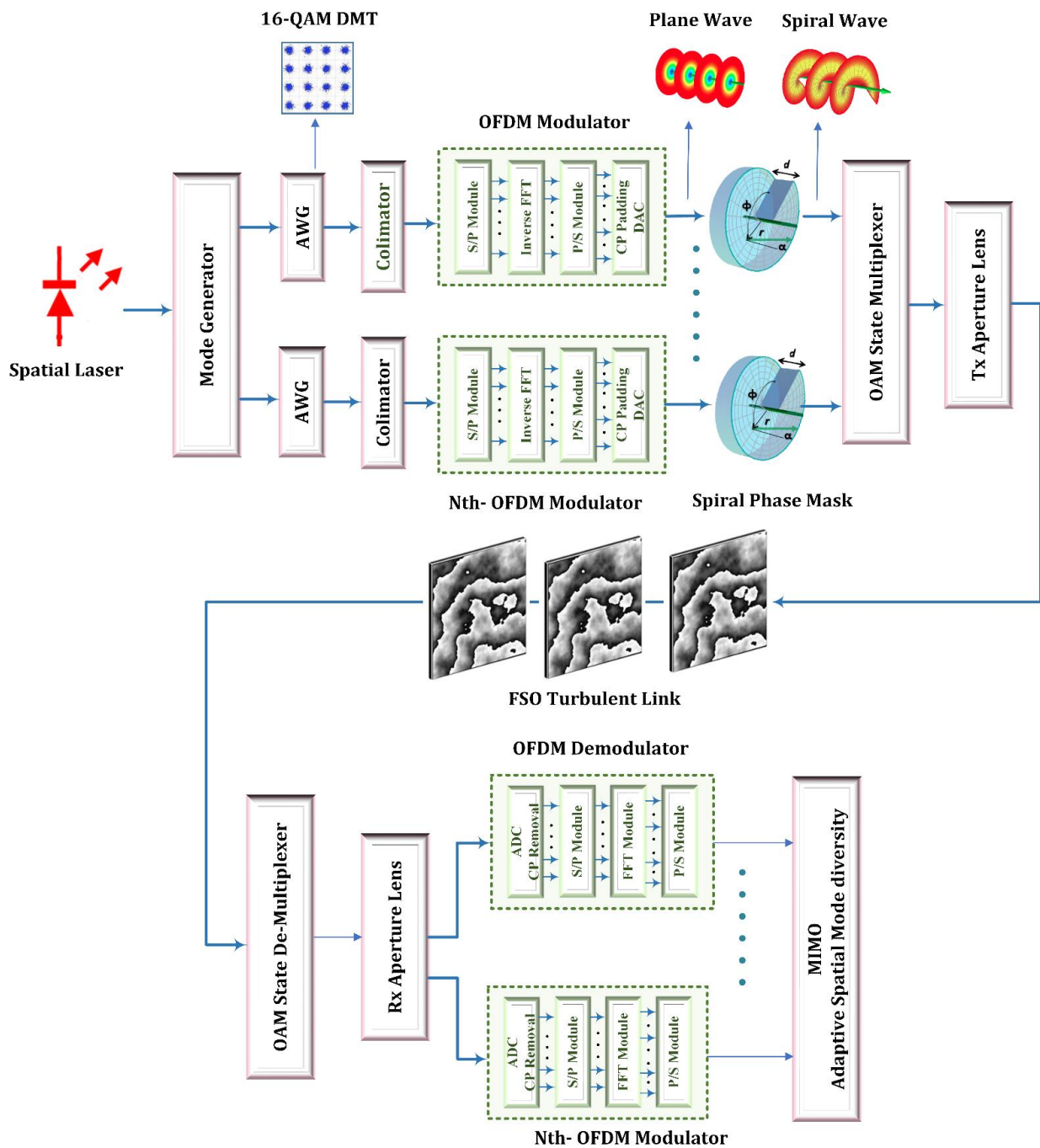


Figure 2. Schematic of the OAM-OFDM-SMM-MIMO spatially multiplexed FSO system.

In Figure 1, the collimated Gaussian laser beams are produced to carry independent and orthogonal data streams at a wavelength of 1550 nm. Spiral phase mask (SPM) converts the high-speed 120 Gbps binary data into OAM mode division multiplexed (OMDM) signal. These OAM spatially multiplexed (SMM) beams are transmitted through a pair of transmitter lenses having  $f_1$  and  $f_2$  focal lengths, respectively, before transmitting over the turbulent transmission link. The equivalent focal length of this pair of lenses is given by

$$\frac{1}{f_0} = \frac{1}{f_1} + \frac{1}{f_2} - \frac{d_f}{f_1 f_2} \tag{1}$$

where,  $\Delta = f_1 + f_2 - d_f$  is the lens offset and  $d_f$  is the center-to-center lens spacing.

Through the careful design and adjustment of this lens pair offset, we can not only focus the transmitted OAM beams at the receiver end, but also help to minimize the transmitted signal power losses. This also makes the OAM-multiplexed FSO link robust against pointing error [15].

As shown in Figure 2, the OAM-OFDM-SMM-MIMO FSO optical transmitter consists of  $N$  independent OFDM subsystems. A 16-QAM-modulated real-valued discrete multi-tone (DMT) electrical signal is produced by a random waveform generator (AWG) at a sample rate of 25 G samples per second. These signals are further modulated in the OFDM modulation subsystems and multiplexed with different orthogonal OAM states. These  $M = 65,615$  subcarriers, are used to transmit the data, with the effective bandwidth of 9.72 GHz of the DMT signal. A cyclic prefix of 40 samples is padded in front of each DMT signal.

The  $j_{th}$  OAM states are chosen from the set  $S = \{-K, -K + 1 \dots 0 \dots K, K + 1\}$  with the  $K$  as the maximum OAM state and the  $j_{th}$  of the OFDM modules is associated with this OAM states set. Total number of orthogonal OAM states generated are given by  $L = 2K + 1$  corresponding to OFDM symbols and, hence, share the same frequency spectrum in the OAM-OFDM-SMM-MIMO FSO system. These frequency channels are further multiplexed to enhance the spectrum efficiency of the proposed system. The frequency  $f_m$  of the  $m_{th}$  OFDM subcarrier in each OFDM module is chosen from  $F = \{f_0, f_2, \dots, f_m, \dots, f_{M-1}\}$  and given by

$$f_m = \frac{m}{T_s} + f_{sc} \text{ for } 0 \leq m \leq M - 1 \tag{2}$$

where,  $T_s$  and  $f_{sc}$  are the symbol period and minimum subcarrier frequency, respectively. In the  $j_{th}$  OFDM subsystem, S/P block converts a set of serial symbols into low data rate  $M$  parallel symbols. Further, the  $m_{th}$  parallel symbol is modulated in frequency domain signal  $X_m^j$  and later this symbol is again transformed to a time domain signal  $S_m^j$  in an inverse.

Fourier transform (IFFT) block. Further, the P/S module converts the  $M$  parallel time domain signal  $S_m^j(t)$  to a serial signal  $S_{OFDM}^j(t)$ , which is expressed as

$$S_{OFDM}^j(t) = \sum_{m=0}^{M-1} X_m^j e^{2\pi i f_m t} \tag{3}$$

The transmitted OAM-OFDM-SMM multiplexed signal after adding a cyclic prefix (CP) into a  $S_{OFDM}^j$  signal and converting it into an analog signal in the DAC module corresponding to the  $u_{th}$  mode states for  $1 \leq u_{th} \leq U$  is given in matrix form by Equation (4):

$$S_{OAM-OFDM}(t) = \sum_{j=1}^L \sum_{u=0}^{U-1} \sum_{m=0}^{M-1} X_m^j e^{2\pi i f_m t} e^{\frac{2\pi i u l_j}{U}} \tag{4}$$

$$S = S_{OAM-OFDM}(t) = [S_1(n), S_2(n) \dots \dots \dots, S_N(n)]^T \tag{5}$$

When this signal shown by Equation (5) is transmitted through the turbulent FSO channel, a phase distorted signal  $\hat{S}$  is received at the optical receiver end and given by

$$\hat{S} = [\hat{S}_1(n), \hat{S}_{21}(n) \dots \dots \dots, \hat{S}_N(n)]^T = HS \tag{6}$$

The plane wave from the output of the OAM state de-mux subsystem is demodulated in the  $j_{th}$  OFDM demodulator subsystem using the inverse process used in the OFDM modulator subsystem. Thus, the output signal matrix from the de-multiplexer and OAM state converter is expressed by [16].

$$Y = [Y_1(n), Y_2(n), \dots \dots \dots Y_N(n)] = G\hat{S} \tag{7}$$

where  $H$  and  $G$  are the  $N \times N$  atmospheric turbulence channel and OAM-OFDM-SMM MIMO matrix respectively with  $h_{i,j} \in H, g_{i,f} \in G$  and  $i,j \in N$ . The estimation SNR for the

tap gain coefficient  $w_{ij}^l$  of length  $L + 1$  for the spatial mode multiplexed equalization is expressed as

$$\hat{y}_j(n) = \sum_{i=1}^N \sum_{l=0}^L w_{ij}^l \hat{s}_i(n-l) \tag{8}$$

### 3. Concept of Spatial Mode Diversity

A spatial mode multiplexed (SMM) beam for the proposed system is generated using a spatial phase mask (SPM) and is expressed by

$$U(\omega_z, \varphi) = A(\omega_z) e^{i\varphi} \tag{9}$$

where,  $A(\omega_z) \propto e^{(-\frac{\omega_z}{\omega_0})}$  is the electric field strength of the Gaussian beam of waist radius of  $\omega_z$  at the transmission distance  $z$  and  $\omega_0$  at  $z = 0$  respectively. The OAM state phase difference is defined by  $\varphi$ . After 16-QAM modulation, the hybrid electric field distribution of  $N$ , OAM-OFDM state, spatially multiplexed signal [17] is given by

$$U_{Mux}(\omega_z, \phi, t) = \sum_{s=1}^N m_s(t) A_s(\omega_z) e^{i l_s \phi_L} \tag{10}$$

In above expression,  $m_s(t)$  is the 16-QAM modulated signal and  $l_s$  is the topological quantum number which is distinctive by the angle mark of ‘ $s$ ’ respectively. The total power in  $k_{th}$  symmetrical OAM mode state Gaussian beam  $g(t)$  is given by  $r_k = P_{+m} + P_{-m}$  and the power ratio  $\alpha_N$  of  $m_{th}$  specific beam to the total power is expressed by  $\alpha_N = \frac{\sqrt{P_{+m}}}{r_k}$ . The coherent coupling in the optical light field [18] for the relative phase shift  $\phi_L$  between two OAM beams is given by

$$S_{KNL}(r_k, \alpha_N, \phi_L, t) = U_1(r_k, \alpha_N, \phi_L, t) + U_2(r_k, \alpha_N, \phi_L, t) = \sqrt{r_k g(t) \alpha_N^2} e^{im\theta} e^{(-\frac{i\phi_L}{2} g(t))} + \sqrt{r_k g(t) (1 - \alpha_N^2)} e^{-im\theta} e^{(\frac{i\phi_L}{2} g(t))} \tag{11}$$

A generalized Laguerre–Gaussian ( $LG_{p,l}$ ) beam of twisted photons [19] with wavelength  $\lambda$ , angular momentum  $l$ , and radial mode number  $p$  is characterized by Equation (12), whereas the received field is given by the Equation (13), respectively:

$$\omega_z = \omega_0 \sqrt{(2p + l + 1) \left( 1 + \left( \frac{\lambda z}{\pi \omega_0^2} \right)^2 \right)} \tag{12}$$

$$\phi(r, z) = \sum_{i=-\infty}^{+\infty} \sum_k \rho_k \alpha_{ki} u_i(r, z) \tag{13}$$

After spatial mode de-multiplexing and the photo-detector collecting process, the received power in the  $i_{th}$  channel state of OAM mode [20] is given by

$$y_i = \int \left| \sum_{k \in N} \rho_k \alpha_{ki} u_i(r, z) \right|^2 dr = \sum_{k \in N} \rho_k \alpha_{ki} \tag{14}$$

As stated in Equation (14), the signal and the inter-channel crosstalk (ICC) are coherently superimposed for the proposed system. Here  $\alpha_{ki}$  refers to the complex coefficient between the  $k_{th}$  transmitted and  $i_{th}$  received mode state of the instantaneous channel state, whereas ‘ $r$ ’ refers to the position vector. Hence the received signal vector field can be expressed as

$$Y = [Y_1, Y_2, \dots, Y_N]^T = Y = |H_\rho|^2 = \left| \begin{bmatrix} \alpha_{11} & \dots & \alpha_{N1} \\ \vdots & \dots & \vdots \\ \alpha_{1N} & \dots & \alpha_{NN} \end{bmatrix} \right|^2 \tag{15}$$

where,  $\rho = [\rho_1, \rho_2, \dots, \rho_N]^T$  is the transmitted signal vector, and  $H$  is the channel matrix consists of  $\alpha_{i,j}$  coefficients, respectively. This non-linear transformation between the  $N$  number of transmitted and received spatial mode signals is caused by square law detection, which is used in conventional MIMO digital signal processing techniques [21]. The photon rate  $A_i$  of this channel for the photon detector efficiency  $\mu$  and signal  $\rho_i \alpha_{ii}$ , calculated from the SMM [20], can be written in the expression below. The following expression can be used to express the photon rate  $A_i$  of this channel for the photon detector efficiency  $\mu$ . Here,  $\rho_i \alpha_{ii}$ , shows the signal from the calculated SMM [20].

$$A_i = \mu |\rho_i \alpha_{ii} + \sum_{k \in N, K \neq i} \rho_k \alpha_{ki}|^2 \tag{16}$$

During our analysis, we assume that the channel state information for the signal amplitude fading  $|\alpha_{ii}|$  at the receiver end is estimated by collecting the received power and exciting the  $i_{th}$  spatial multiplexed mode. In this case  $\rho_i \alpha_{ii}$  is obtained directly from the spatial mode multiplexing calculations.

The photon rate obtained from Equation (16) is a half normal distribution, whose intensity fluctuation is represented by a probability density function (pdf) under atmospheric turbulence conditions. The results obtained from Equations (15) and (16) are used in calculations of probability density function as well as the channel capacity given by the Equations (27) and (28) in Section 4, respectively. The instantaneous asymptotic optical signal-to-noise ratio [20] (OSNR) can be calculated by using Equation (17). Each channel in the proposed system carries high-speed, 16-QAM modulated information, resulting in  $N$  multiplexed OAM channels. The probability of error of the 16-QAM modulation [22] under atmospheric turbulence is given by

$$\gamma_i = \frac{|\alpha_{ii}|^2}{\sum_{k \in N, K \neq i} E[|\alpha_{ki}|^2]} \tag{17}$$

$$P_e = 3Q \left( \sqrt{\frac{4E_{avg}}{5N_0}} \right) \left[ 1 - 0.75Q \sqrt{0.8 \frac{E_{avg}}{5N_0}} \right] \tag{18}$$

where,  $N_0$  and  $Q(\cdot)$  are the FSO link's noise power spectral density and complementary error function, respectively.

The received field strength for the  $i_{th}$  spatially multiplexed signal [20] at the received plane for the Lagrange Gaussian (LG) polynomial  $L_0^i$  is expressed by

$$u_{i*}(\omega_z, \phi, 0) = \sqrt{\frac{2}{\pi|i|}} \frac{1}{\omega_0} \left( \frac{\sqrt{2}\omega_z}{\omega_0} \right)^{|i|} L_0^i \left( \frac{2\omega_z^2}{\omega_0^2} \right) e^{-\left(\frac{\omega_z^2}{\omega_0^2} + j\phi\right)} \tag{19}$$

#### 4. Capacity Modelling of the Proposed System

Turbulence-induced scintillation is the major factor that can impact the propagation of a spatial mode multiplexed signal across the FSO link [23]. These scintillation distortions are produced due to local fluctuations in pressure and temperature in the atmosphere. This random change in the atmospheric refractive index results in the leakage of signal power from one mode to adjacent modes. This phenomenon results in modes overlapping with power penalties.

The scintillation theory states that the intensity fluctuations of the received OAM-OFDM-SMM multiplexed signal  $I = x \times y$  is the product of large ( $\alpha$ ) and small ( $\beta$ ) scale turbulent eddies in GG turbulence conditions of the atmospheric channel. These intensity fluctuations are represented by the conditional PDF corresponding to  $\alpha$  and  $\beta$  parameters at the system receiver end by Equations (20) and (21) respectively [24]. Here the Rytov

constant is given by  $\sigma^2 = 1.23C_n^2 k^{7/6} z^{11/6}$  and  $C_n^2$  is the refractive structure parameter whereas  $\Gamma(\cdot)$  denote the Gamma function.

$$f_x(x) = \frac{\alpha(\alpha x)^{\alpha-1}}{\Gamma\alpha} e^{-\alpha x} \text{ for } x, \alpha > 0 \tag{20}$$

$$f_y(y) = \frac{\beta(\beta y)^{\beta-1}}{\Gamma\beta} e^{-\beta y} \text{ for } y, \beta > 0 \tag{21}$$

$$\alpha = \left( \exp \left[ \frac{0.49\sigma^2}{(1 + 1.11\sigma^{2.4})^{7/6}} \right] - 1 \right)^{-1} > 0 \tag{22}$$

$$\beta = \left( \exp \left[ \frac{0.51\sigma^2}{(1 + 0.691\sigma^{2.4})^{5/6}} \right] - 1 \right)^{-1} > 0 \tag{23}$$

The conditional PDF of intensity fluctuation  $I$  for the fixed values of  $x$  is further expressed by Equation (24), whereas the unconditional PDF can be further derived by taking the average of this Equation (24) over the Gamma distribution using Equation (20). Finally, the PDF for the GG distribution function can be derived for the modified Bessel function  $K(\cdot)$  of second kind and written by Equation (25).

$$f_y(I/x) = \frac{\beta(\beta I/x)^{\beta-1}}{x\Gamma\beta} e^{-(\beta I/x)} \tag{24}$$

$$f(I) = \frac{2(\alpha\beta)^{(\alpha+\beta)/2}}{\Gamma\alpha\Gamma\beta} I^{(\alpha+\beta)/2-1} K_{\alpha-\beta} \sqrt{2\alpha\beta I} \tag{25}$$

Considering Equation (25), and the bit error rate (BER) equation for the orthogonal modulation scheme [22], the BER of the OAM-OFDM signal, for the transmitted and received OAM state,  $l_q$  and  $l$  and  $m_{th}$  subcarrier frequency, is given by

$$\langle ber_{l,m} \rangle = \int_0^\infty 0.5 f_I(I) \operatorname{erfc} \sqrt{\frac{I^2 \gamma_{l,m}}{2}} dI \tag{26}$$

In the above Equation (26),  $f_I(I)$ , represents the PDF of the intensity fluctuation of the OFDM signal at the receiver end due to atmospheric turbulence, whereas,  $\gamma_{l,m} = \frac{P_{l,m}(l,z)}{\sum_{l_q \neq l} P_{l,m}(l_q,z) + P_{l,q}^{N_0}}$  denotes the signal-to-noise ratio (SNR) of the OAM-OFDM channel for the transmitted power  $P_{tx}$  and,  $\operatorname{erfc}(\cdot)$  is the complementary error function [25].

In this proposed FSO system, a binary symmetric channel (BSC) is adopted, whose transmission channel capacity is derived in Refs. [7,26]. Hence the capacity of the OAM-OFDM FSO system can be expressed by Equation (27)

$$C(\langle ber_{l,m} \rangle) = 1 + \langle ber_{l,m} \rangle \log_2 \langle ber_{l,m} \rangle + (1 - \langle ber_{l,m} \rangle) \log_2 (1 - \langle ber_{l,m} \rangle) \tag{27}$$

hence, the total capacity of OAM-OFDM-SMM multiplexed FSO transmission systems can be expressed as

$$C = \sum_{l=-K}^{+K} \sum_{m=0}^{M-1} C(\langle ber_{l,m} \rangle) \tag{28}$$

### 5. Numerical Results and Discussion

In this section, the BER and channel transmission capacity performances of the proposed OAM-OFDM-SMM multiplexed MIMO FSO system are evaluated with respect to various performance metrics, such as the number of OAM states, various refractive index structure parameters, Rytov parameters, different FSO link distances, and different signal-

to-power ratios (SNR) under various weak to strong atmospheric channel conditions. In the optical transmitter section, the OAM states are multiplexed to carry OAM-OFDM-SMM multiplexed channels, where each channel is 16-QAM modulated and carries information at a data speed of 120 Gb/s over a wavelength of 1550 nm. Equation (28) is used to calculate the minimum power required/channel to achieve a set target BER.

To analyze the performance of the proposed system, the following assumptions are also made: (i) the system physical and default parameters used to calculate and evaluate the proposed FSO system are summarized in Table 1; (ii) transmitted power for all the channels is kept equal; (iii) the forward error correction (FEC) limit is set to be  $3.8 \times 10^{-3}$  corresponding to threshold SNR of 18 dB; (iv) inter-channel crosstalk with the signal behaves similarly to noise at our BER threshold; and (v) the large-scale eddies and small-scale eddies are represented by  $\alpha_{rj,m}$  and  $\beta_{rj,m}$ , respectively.

**Table 1.** Physical parameters for the proposed system.

System Parameters	Symbol	Simulation Values
Spatial laser power	$P_l$	−15 dBm
Bit rate per channel	$R_b$	120 Gb/s
Number of OAM modes	$L$	21
Maximum OAM state	$K$	10
Lens focal length	$f_1 = f_2$	50 cm
Transmitted wavelength	$\lambda$	1550 nm
Transmitter Power	$P_t$	15 dBm
Maximum RIS onstant	$C_n^2$	$1 \times 10^{-15} \text{ m}^{-2/3}$
Maximum Rytov constant	$\sigma^2$	3.98
Number of subcarriers	$f_{sc}$	65615
Minimum subcarrier frequency	$f_{sc}$	30 GHz
Subcarrier interval	$\Delta f$	1 KHz
Gaussian beam size	$\omega_0$	30 cm
Maximum FSO link distance	$z$	2 km
Receiver losses	$L_{rx}$	0 dB
Photo-detector responsivity	$R$	1 A/W
Detector dark current	$I_0$	10 nA
Thermal noise power density	$\eta$	$10^{-22} \text{ W/Hz}$

The simulation results for the intensity profile and phase front distortion of the purest OAM-OFDM-SMM-MIMO mode  $l = +1$  are illustrated in Figure 3 under weak ( $C_n^2 = 1.0 \times 10^{-10} \text{ m}^{-2/3}$  and  $(\sigma^2 < 1)$ ) and under strong atmospheric turbulence ( $C_n^2 = 1.0 \times 10^{-15} \text{ m}^{-2/3}$  and  $(\sigma^2 > 1)$ ) conditions for the link distance of 1 km, respectively. For the purest mode, the beam waist parameter is  $\omega_0 = 1 \text{ m}$ . In very weak AT, there is almost no phase front distortion, most of the transmitted power remains in OAM = +1 mode, and almost negligible optical power leakage occurs from this mode to other adjacent modes. However, under severe AT conditions, we clearly observe the EM field's distorted phase front, which causes a high-power leakage to other modes. At the receiver end, the normalized power received for 7 different OAM modes is also shown in Figure 3. The normalized received power for  $l = +1$  mode under strong AT conditions decreases by almost 10 dB compared to weak AT conditions, whereas  $l = -3$  mode demonstrates the worst performance profile under the same conditions.

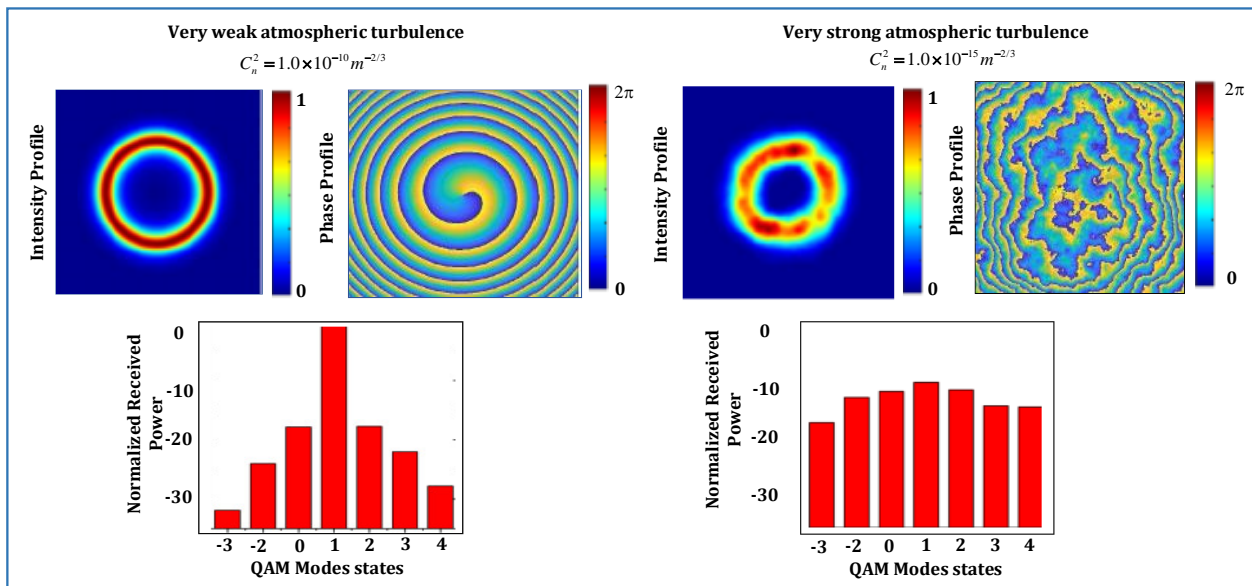


**Figure 3.** Intensity and phase profiles of OAM state in different turbulence regions.

Figure 4 illustrates the BER vs. number of OAM mode states for four different refractive index structure (RIS) parameters from  $[4 \times 10^{-12}] m^{-2/3}$  to  $[6 \times 10^{-12}] m^{-2/3}$  atmospheric turbulence conditions. These turbulence conditions correspond to strong and weak atmospheric turbulences. Due to the severe vulnerability of the higher-order OAM states in different turbulence conditions, the BER curve increases with the increase in absolute value of the OAM state for the fixed value of the refractive index structure parameter. The result obtained demonstrates that the BER curve is symmetrical with respect to the different OAM states and that the center is located at the zero mode state. When the RIS parameter is kept constant for any turbulence conditions, the BER performance curve increases almost in a linear manner with the increase in the absolute value of the low-order OAM mode state maximum up to the OAM state of  $-17$ , whereas for the absolute value of higher-order OAM mode states beyond  $-17$ , the BER performance curve decreases gradually with the increase in OAM mode order. This is mainly due to mode energy leakage or spreading in adjacent OAM modes. For the mode state from  $-3$  to  $0$ , the BER performance remains almost constant. The symmetrical BER performance is observed for the OAM mode state from  $0$  to  $20$ . When the OAM mode state is kept constant, it is observed that the BER increases with the increase in the RIS structure constant value due to the decrease in atmospheric turbulence strength.

The BER performances of the OAM-SMM-MIMO and OAM-OFDM-SMM-MIMO FSO systems are compared in Figure 5 with respect to different OAM states during atmospheric turbulence. When the OAM state value is maintained constant, the BER of the OAM-OFDM-SMM-MIMO FSO system is significantly higher than the BER of the straightforward OAM-SMM FSO transmission system. The results distinctively show that atmospheric turbulence has an effect on the performance of both FSO systems; however, the variations in received OFDM-MIMO/SMM signals are primarily affected by intensity variations, as opposed to the impact of atmospheric turbulence on OAM signals, which is primarily caused by phase distortion or variations. Due to the fact that OFDM signals are also impacted by atmospheric turbulence, the OAM-OFDM-SMM FSO system is more adversely affected than OAM signals.

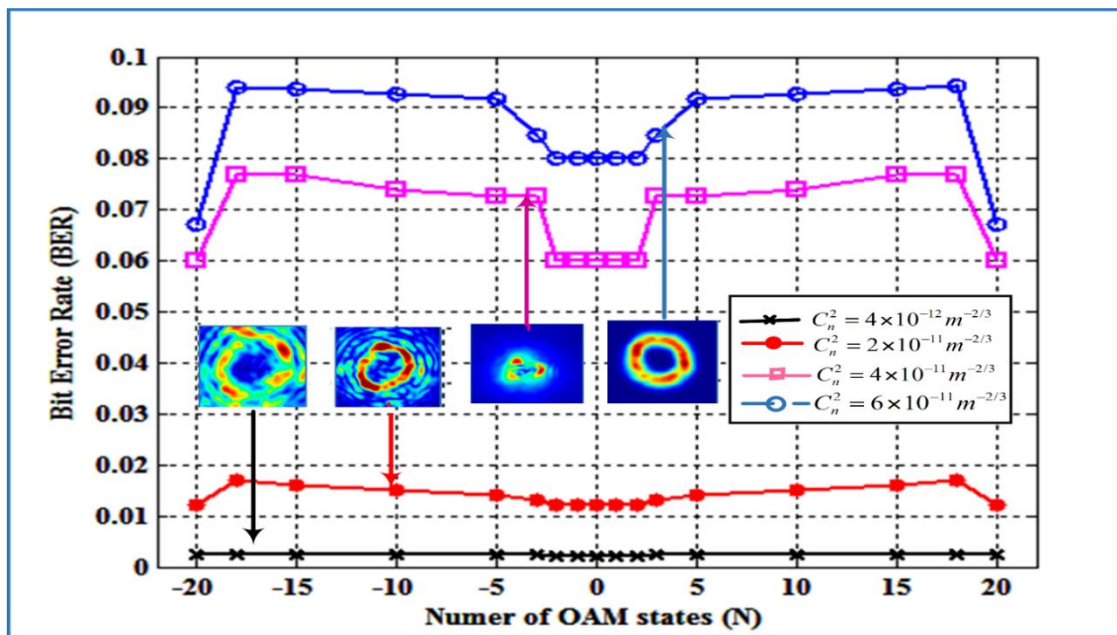


Figure 4. BER vs. OAM states under different refractive index structure parameters.

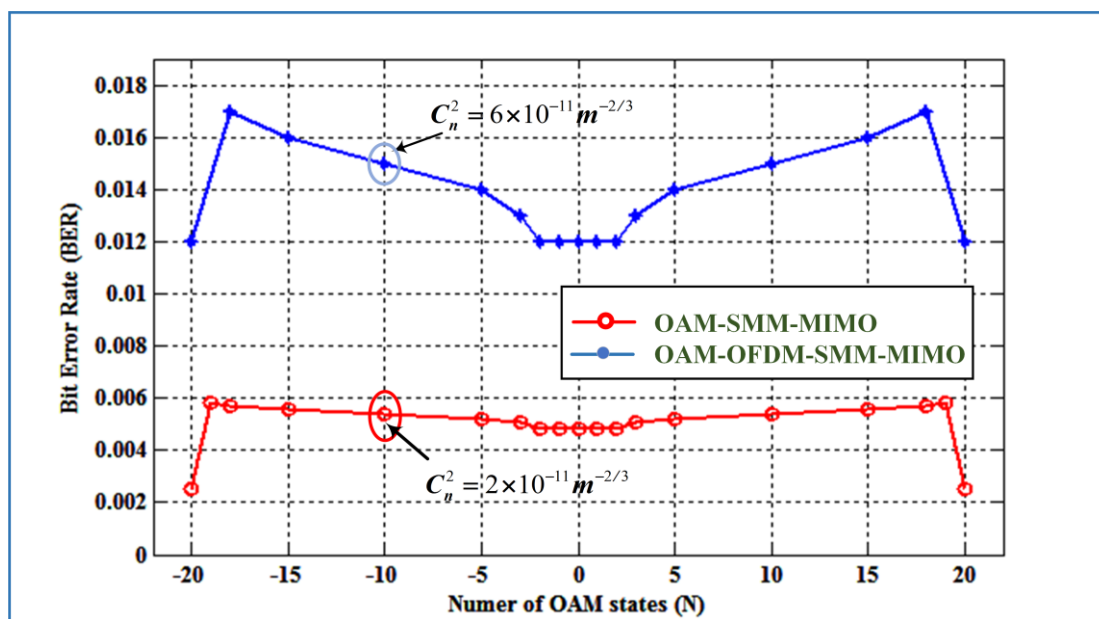


Figure 5. BER vs. OAM state for the OAM-SMM-MIMO and the OAM-OFDM-SMM-MIMO FSO systems.

The BER performance of the proposed system is compared as a function of different order OAM mode states in Figure 6 for three different link distances, from a maximum of 2 km to a minimum of 0.75 km, respectively, in atmospheric turbulence. When the order of the OAM state is kept constant, say at 0, the BER increases with an increase in optical link distances. The plot validates the fact that with an increase in optical link distances, both the atmospheric attenuation and the turbulence become stronger, which ultimately leads to a higher numerical value of BER and hence the worst system performance. The proposed system performs admirably for lower-order OAM states with absolute values ranging from 0 to 5 over a propagation distance of 0.75 km, but it performs poorly for the same order of OAM modes over a distance of 2 km. This is because of the least spreading of lower-order OAM state modes' energy, which is the minimum leakage of the mode energy from one mode to adjacent OAM modes.

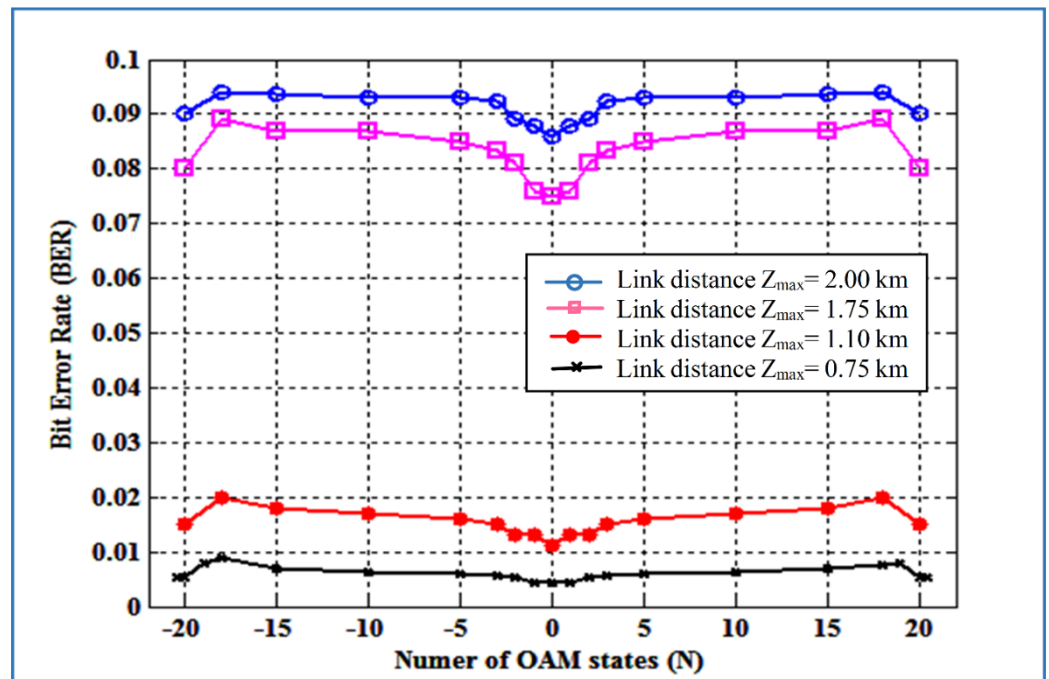


Figure 6. BER vs. OAM states for different optical link distances.

Figure 7 compares the BER performance as a function of increasing OSNR values for the two OAM-SMM-MIMO and OAM-OFDM-SMM MIMO FSO systems, considering the intensity fluctuations at the receiver, respectively. For the performance analysis, a fixed and moderate atmospheric turbulence with a RIS parameter of  $2 \times 10^{-12} \text{ m}^{-2/3}$  and the OAM  $l = +1$  state mode is assumed. We observe that the BER graphs decrease exponentially with the increasing value of OSNR from 0 to 30 dB and cross the set FEC threshold limit of  $3 \times 10^{-3}$  at 20 dB and 24.1 dB for both of these systems, respectively. The OAM-SMM based MIMO FSO system clearly demonstrates the superior performance over the OAM-OFDM-SMM based FSO system. This also validates the concept that both systems are influenced by atmospheric turbulence due to intensity fluctuations; however, this effect on the OAM-SMM based MIMO FSO system is less than that on the OAM-OFDM based MIMO FSO system. For the chosen threshold value of  $3.8 \times 10^{-3}$ , the OAM-SMM based system requires a 4.1 dB lesser amount of power compared to the OAM-OFDM based FSO system. At OSNR value of 25 dB, the performance of the OAM based system is approximately 100 times better than OFDM based SMM MIMO FSO system. Both the FSO systems can perform excellently below the set BER threshold for higher OSNR values beyond 23.5 dB.

The performance of the proposed system is also compared for log BER vs. OSNR ranging from 2 to 35 dB for GG turbulence conditions and different numerical values of the Rytov constant as shown in Figure 8. It can be seen from the plots that as the numerical value of the Rytov constant  $\sigma^2$  decreases from 3.98 to 0.83, the atmospheric turbulence becomes weaker, resulting in an excellent proposed system log BER performance. For the fixed value of OSNR at 20 dB, the log BER are  $-3.28$ ,  $-2.91$ , and  $-2.55$ , corresponding to  $\sigma^2 = 0.83$ , 1.81, and 3.98, respectively.

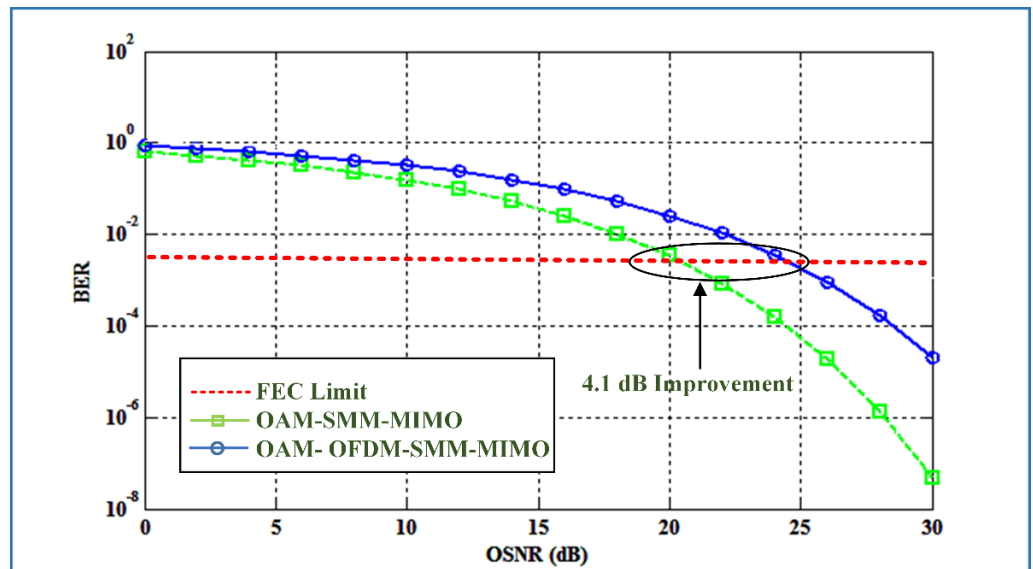


Figure 7. BER vs. OSNR for  $l = +1$  OAM mode and OFDM SMM FSO system.

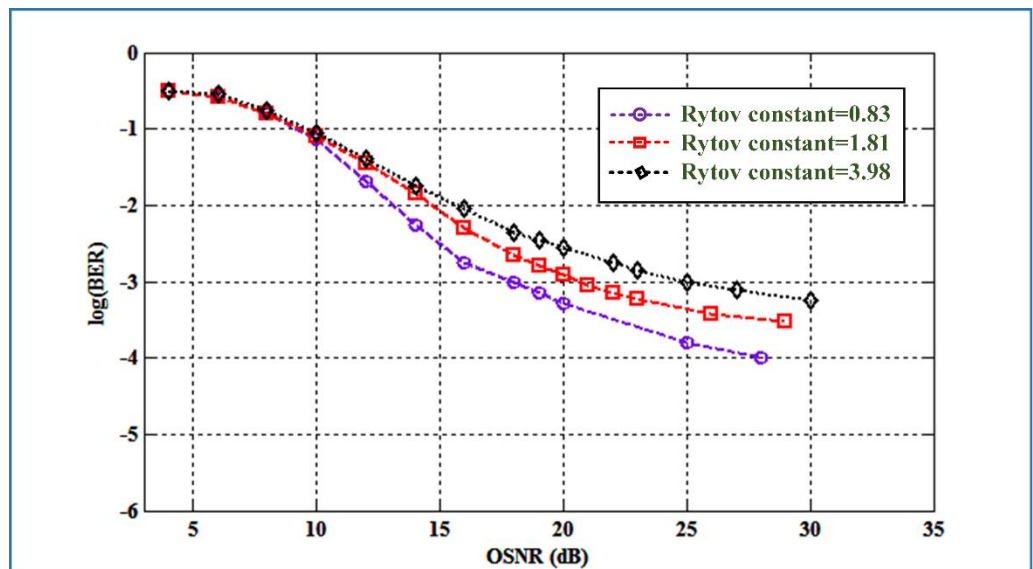
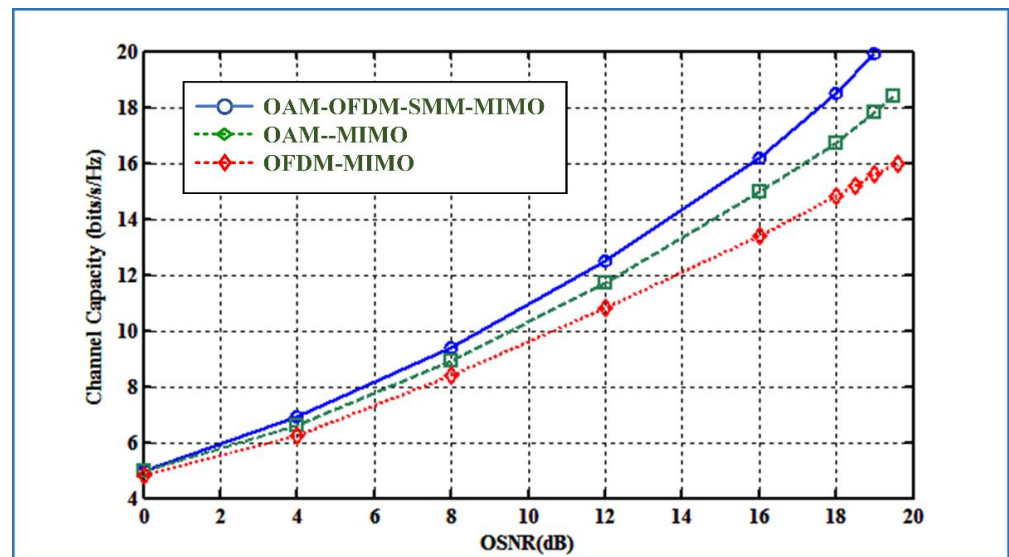


Figure 8. BER vs. OSNR for different Rytov constants under GG turbulence.

Figure 9 demonstrates the increase in channel capacity with respect to the function of different OSNRs (dB) for the three FSO systems, OFDM-MIMO, OAM-MIMO, and OAM-OFDM-SMM-MIMO, respectively, under turbulence conditions  $(2 \times 10^{-12}) \text{ m}^{-2/3}$ . It is observed from the graph that the OAM-OFDM-MIMO FSO system for OAM state  $l = +1$  and the 8 OFDM subcarrier based on SMM outperforms compares to the other two conventional MIMO-FSO systems. At 18 dB OSNR, the channel capacity offered by the proposed OAM-OFDM-SMM-MIMO system is nearly 3.3 bits/s/Hz better than a simple OFDM-MIMO system and 1.6 bits/s/Hz better than an OAM-OFDM-SMM based MIMO FSO transmission system. When the channel capacity was set to 14 bits/s/Hz, the proposed OAM-OFDM-MIMO FSO system based on SMM required nearly 3.2 dB less power than OFDM-MIMO and 1.1 dB less power than the OAM-MIMO FSO system. The result clearly validates that by combining OAM and OFDM along with the spatial mode diversity scheme, one can enhance the capacity of the FSO transmission system. We present a novel approach to increasing channel capacity while also increasing diversity gain.



**Figure 9.** Channel capacity vs. OSNR for the conventional OAM and the proposed system.

## 6. Conclusions and Future Work

In this article, we have analyzed the high-speed, enhanced transmission capacity OAM-OFDM-SMM FSO system, which combines the advantages of OAM multiplexing and OFDM techniques with MIMO spatial mode diversity schemes in the existing OAM and OFDM, MIMO FSO communication system to investigate the performance of the system under turbulence conditions. Furthermore, the proposed OAM-OFDM-SMM based MIMO-FSO system is a multi-transmission optical link system that exploits the spatial dimensions of laser beams to design a reliable crosstalk FSO model under the impact of atmospheric turbulence to increase the spectral efficiency and diversity gain. Moreover, the numerical results obtained from the simulations illustrate that the proposed OAM-OFDM FSO system, based on spatial mode diversity, has effectively improved the performance of the FSO communication link using spatial mode diversity in various atmospheric turbulence conditions. The BER and the capacity performances of the proposed system have been compared for various parameters such as number of OAM states, link distance, OSNR, and RIS. Although the proposed system can also be investigated for parameters such as power penalty calculation for intermodal crosstalk, received power vs. angular receiving aperture, and outage probability for transmitted power. The link distance needs to be increased while keeping the speed and the channel capacity constant.

We can also improve the performance of the existing work and propose a new OAM-OFDM-SMM, MIMO FSO communication system in the future by incorporating different channel coding techniques, multiplexing techniques such as dense wavelength division multiplexing (DWDM), various turbulence compensation techniques, and the CSI model to improve the channel capacity enhancement of the proposed FSO system. Also, we can exploit the performance of the proposed system for different OFDM subcarriers' under various refractive index structure constants to analyze the capacity of the FSO system.

**Author Contributions:** Methodology, A.A., M.S., M.A. and K.A.; Writing—original draft, S.S.; Writing—review & editing, C.K. All authors have read and agreed to the published version of the manuscript.

**Funding:** This research received no external funding.

**Institutional Review Board Statement:** Not Applicable.

**Informed Consent Statement:** Not Applicable.

**Data Availability Statement:** Not Applicable.

**Conflicts of Interest:** The authors declare no conflict of interest.

## References

1. Gibson, G.; Courtial, J.; Padgett, M.J.; Vasnetsov, M.; Pas'ko, V.; Barnett, S.M.; Franke-Arnold, S. Free-space information transfer using light beams carrying orbital angular momentum. *Opt. Express* **2004**, *12*, 5448–5456. [[CrossRef](#)]
2. Yao, A.M.; Padgett, M.J. Orbital angular momentum: Origins, behavior and applications. *Adv. Opt. Photonics* **2011**, *3*, 161–204. [[CrossRef](#)]
3. Hu, T.; Wang, Y.; Liao, X.; Zhang, J.; Song, Q. OFDM-OAM modulation for future wireless communications. *IEEE Access* **2019**, *7*, 59114–59125. [[CrossRef](#)]
4. Wang, J.; Yang, J.-Y.; Fazal, I.M.; Ahmed, N.; Yan, Y.; Huang, H.; Ren, Y.; Yue, Y.; Dolinar, S.; Tur, M.; et al. Terabit free-space data transmission employing orbital angular momentum multiplexing. *Nat. Photonics* **2012**, *6*, 488–496. [[CrossRef](#)]
5. Huang, H.; Xie, G.; Yan, Y.; Ahmed, N.; Ren, Y.; Yue, Y.; Rogawski, D.; Willner, M.J.; Erkmen, B.I.; Birnbaum, K.M.; et al. 100 Tbit/s free-space data link enabled by three-dimensional multiplexing of orbital angular momentum, polarization, and wavelength. *Opt. Lett.* **2014**, *39*, 197–200. [[CrossRef](#)]
6. Ge, X.; Zi, R.; Xiong, X.; Li, Q.; Wang, L. Millimeter Wave Communications with OAM-SM Scheme for Future Mobile Networks. *IEEE J. Sel. Areas Commun.* **2017**, *35*, 2163–2177. [[CrossRef](#)]
7. Wang, L.; Ge, X.; Zi, R.; Wang, C.-X. Capacity Analysis of Orbital Angular Momentum Wireless Channels. *IEEE Access* **2017**, *5*, 23069–23077. [[CrossRef](#)]
8. Xie, G.; Li, L.; Ren, Y.; Huang, H.; Yan, Y.; Ahmed, N.; Zhao, Z.; Lavery, M.; Ashrafi, N.; Ashrafi, S.; et al. Performance metrics and design considerations for a free-space optical orbital-angular-momentum-multiplexed communication link. *Optica* **2015**, *2*, 357–365. [[CrossRef](#)]
9. Yan, Y.; Xie, G.; Lavery, M.P.J.; Huang, H.; Ahmed, N.; Bao, C.; Ren, Y.; Cao, Y.; Li, L.; Zhao, Z.; et al. High-capacity millimetre-wave communications with orbital angular momentum multiplexing. *Nat. Commun.* **2014**, *5*, 4876. [[CrossRef](#)]
10. Huang, H.; Cao, Y.; Xie, G.; Ren, Y.; Yan, Y.; Bao, C.; Ahmed, N.; Neifeld, M.A.; Dolinar, S.J.; Willner, A.E. Crosstalk mitigation in a free-space orbital angular momentum multiplexed communication link using 4x4 MIMO equalization. *Opt. Lett.* **2014**, *39*, 4360–4363. [[CrossRef](#)]
11. Ren, Y.; Wang, Z.; Xie, G.; Li, L.; Cao, Y.; Liu, C.; Liao, P.; Yan, Y.; Ahmed, N.; Zhao, Z.; et al. Free-space optical communications using orbital-angular-momentum multiplexing combined with MIMO-based spatial multiplexing. *Opt. Lett.* **2015**, *40*, 4210–4213. [[CrossRef](#)] [[PubMed](#)]
12. Kaushal, H.; Kaddoum, G. Optical Communication in Space: Challenges and Mitigation Techniques. *IEEE Commun. Surv. Tutorials* **2016**, *19*, 57–96. [[CrossRef](#)]
13. Ciaramella, E.; Arimoto, Y.; Contestabile, G.; Presi, M.; D'Errico, A.; Guarino, V.; Matsumoto, M. 1.28 terabit/s (32x40 Gbit/s) wdm transmission system for free space optical communications. *IEEE J. Sel. Areas Commun.* **2009**, *27*, 1639–1645. [[CrossRef](#)]
14. Sun, X.; Djordjevic, I.B. Physical-layer security in orbital angular momentum multiplexing free-space optical communications. *IEEE Photon. J.* **2016**, *8*, 7901110. [[CrossRef](#)]
15. Li, L.; Xie, G.; Ren, Y.; Ahmed, N.; Huang, H.; Zhao, Z.; Liao, P.; Lavery, M.P.J.; Yan, Y.; Bao, C.; et al. Orbital-angular-momentum-multiplexed free-space optical communication link using transmitter lenses. *Appl. Opt.* **2016**, *55*, 2098–2103. [[CrossRef](#)] [[PubMed](#)]
16. Sun, T.; Liu, M.; Li, Y.; Wang, M. Crosstalk mitigation using pilot assisted least square algorithm in OFDM-carrying orbital angular momentum multiplexed free-space-optical communication links. *Opt. Express* **2017**, *25*, 25707–25718. [[CrossRef](#)]
17. Yang, C.; Xu, C.; Ni, W.; Gan, Y.; Hou, J.; Chen, S. Turbulence heterodyne coherent mitigation of orbital angular momentum multiplexing in a free space optical link by auxiliary light. *Opt. Express* **2017**, *25*, 25612–25624. [[CrossRef](#)]
18. Li, Y.; Morgan, K.; Li, W.; Miller, J.K.; Watkins, R.; Johnson, E.G. Multi-dimensional QAM equivalent constellation using coherently coupled orbital angular momentum (OAM) modes in optical communication. *Opt. Express* **2018**, *26*, 30969–30977. [[CrossRef](#)]
19. Li, L.; Xie, G.; Yan, Y.; Ren, Y.; Liao, P.; Zhao, Z.; Ahmed, N.; Wang, Z.; Bao, C.; Willner, A.J. Power loss mitigation of orbital-angular-momentum-multiplexed free-space optical links using nonzero radial index Laguerre-Gaussian beams. *J. Opt. Soc. USA B Opt. Phys.* **2017**, *34*, 1–6. [[CrossRef](#)]
20. Huang, S.; Mehrpoor, G.R.; Safari, M. Spatial-mode diversity and multiplexing for FSO communication with direct detection. *IEEE Trans. Commun.* **2018**, *66*, 2079–2092. [[CrossRef](#)]
21. Arik, S.; Kahn, J.M. Direct-detection mode-division multiplexing in modal basis using phase retrieval. *Opt. Lett.* **2016**, *41*, 4265–4268. [[CrossRef](#)]
22. Yousif, B.B.; Elsayed, E.E.; Alzalabani, M.M. Atmospheric turbulence mitigation using spatial mode multiplexing and modified pulse position modulation in hybrid RF/FSO orbital-angular-momentum multiplexed based on MIMO wireless communications system. *Opt. Comm.* **2019**, *436*, 197–208. [[CrossRef](#)]
23. Kaur, P.; Jain, V.K.; Kar, S. Performance Analysis of FSO Array Receivers in Presence of Atmospheric Turbulence. *IEEE Photon-Technol. Lett.* **2014**, *26*, 1165–1168.
24. Ghassemlooy, Z.; Popoola, W.; Rajbhandari, S. *Optical Wireless Communications: System and Channel Modelling with MATLAB*; CRC Press: Boca Raton, FL, USA, 2019.

25. Anguita, J.A.; Neifeld, M.A.; Vasic, B.V. Turbulence-induced channel crosstalk in an orbital angular momentum-multiplexed free-space optical link. *Appl. Opt.* **2008**, *47*, 2414–2429. [[CrossRef](#)] [[PubMed](#)]
26. Wang, L.; Jiang, F.; Chen, M.; Dou, H.; Gui, G.; Sari, H. Interference Mitigation Based on Optimal Modes Selection Strategy and CMA-MIMO Equalization for OAM-MIMO Communications. *IEEE Access* **2018**, *6*, 69850–69859. [[CrossRef](#)]

**Disclaimer/Publisher’s Note:** The statements, opinions and data contained in all publications are solely those of the individual author(s) and contributor(s) and not of MDPI and/or the editor(s). MDPI and/or the editor(s) disclaim responsibility for any injury to people or property resulting from any ideas, methods, instructions or products referred to in the content.